NEOPLASIA
www.neoplasia.com

Volume 23 Number 9 September 2021 pp. 887–897

Circ_0089823 reinforces malignant behaviors of non-small cell lung cancer by acting as a sponge for microRNAs targeting SOX4☆,☆☆

Jiwei Li[a]; Zibo Zhu[b]; Saisai Li[a]; Zhijun Han[a]; Fannuo Meng[a]; Li Wei[a,*]

[a] Department of Thoracic Surgery, Zhengzhou Key Laboratory for Surgical Treatment for End-stage Lung Disease, Henan Provincial People's Hospital, Zhengzhou University People's Hospital, Henan University People's Hospital, Zhengzhou, Henan, China.
[b] Department of Thoracic Surgery, Zhengzhou Key Laboratory for Surgical Treatment for End-stage Lung Disease, Zhengzhou University People's Hospital, Henan Provincial People's Hospital, Henan University People's Hospital, Zhengzhou, Henan, China.

Abstract

In recent years, increasing evidence indicates the significant roles of circRNAs in carcinogenesis. However, their roles in lung cancer remain largely unclear. We profiled the circRNA expression in 10 paired non-small cell lung cancer (NSCLC) and adjacent non-cancer tissues using high-throughput sequencing. A total of 183 up-regulated and 428 down-regulated circRNAs were identified in the NSCLC tissues (fold change ≥ 2, $P < 0.05$). Circ_0089823, an up-regulated circRNA (5.4-fold, $P = 0.0017$), was further investigated through loss-of-function and gain-of-function. The circ_0089823 level in NSCLC samples was related to the gender, tumor size, pathological type, TNM stage and smoking history. Knockdown of circ_0089823 suppressed cell proliferation, induced cell cycle arrest and apoptosis of NSCLC cells *in vitro*. Additionally, circ_0089823-silenced xenografts grew much slowly. On the contrary, its over-expression promoted the malignant behaviors of NSCLC cells. Furthermore, SOX4, a tumor-promoting transcription factor, was highly expressed in NSCLC tissues and positively regulated by circ_0089823. Bioinformatic analysis revealed several potential binding sites for miR-507, miR-557, miR-579-3p and miR-1287-5p in circ_0089823 and SOX4 3′-untranslated region, which was later confirmed by luciferase reporter assay. Interestingly, silencing SOX4 countervailed the effects of circ_0089823 over-expression on NSCLC cells. Here, we revealed that circ_0089823 might act as a sponge of microRNAs targeting SOX4, thus increasing the expression of SOX4, thereby reinforcing the malignant behaviors of NSCLC cells. This study indicates that circ_0089823 has the potential to become a candidate target for NSCLC treatment.

Neoplasia (2021) 23, 887–897

Keywords: Circ_0089823, Non-small cell lung cancer, Proliferation, Apoptosis, SOX4, MicroRNA

1 Introduction

Lung cancer is one of the most common malignant carcinomas. There were 2,093,876 new cases (accounting for 11.6% in all cancer cases) and 1,761,007 death (accounting for 18.4% in all cancer-related death) in 2018 worldwide [1]. Despite advancement in lung cancer diagnosis and treatment, its 5-year-survival rate remains less than 16% [2]. Non-small cell lung cancer (NSCLC; including large-cell carcinoma, squamous cell carcinoma and adenocarcinoma) accounts for more than 80% of lung cancer [2]. On account of lacking effective diagnostic biomarkers, NSCLC patients are mainly diagnosed at advanced stages. The outcomes of lung cancer patients with advanced stages are poor [3]. At present, lung cancer is a global public health problem. Therefore, revealing the pathogenesis of lung cancer is vital for developing novel therapeutic strategies.

Circular RNAs (circRNAs) are a class of non-coding RNA, which are generated from precursor mRNA by back-splicing [4]. CircRNAs show a covalently closed loop structure lacking of 5′- or 3′- polarities. They are more stable than their liner transcripts and resistant to RNaseR [5]. In

Abbreviations: ARSE, arylsulfatase E; AUC, area under the curve; CCK-8, cell counting kit-8; circRNAs, circular RNA; DAPI, 4′,6-diamidino-2-phenylindole; FBS, fetal bovine serum; FISH, RNA fluorescence *in situ* hybridization; FITC, fluorescein isothiocyanate; gDNA, genomic DNA; GO, gene ontology; HBE, human bronchial epithelial cells; KEGG, kyoto encyclopedia of genes and genomes; miR, microRNA; NSCLC, non-small cell lung cancer; PI, propidium iodide; qPCR, quantitative real-time PCR; ROC, receiver operating characteristic; SOX4, sex-determining region Y-box 4; TUNEL, terminal deoxynucleotidyl transferase-mediated dUTP nick end labeling; UTR, untranslated region.

* Corresponding author.
E-mail address: facefuture00114321@163.com (L. Wei).

☆ Funding: This study was supported by a grant from the Henan Provincial People's Hospital "23456 Special Research Fund for Talent Project" (No. 011045 and 005820).
☆☆ Conflicts of interests: The authors declare no conflict of interest.
Received 20 March 2021; received in revised form 21 June 2021; accepted 28 June 2021

https://doi.org/10.1016/j.neo.2021.06.011

recent years, a mass of circRNAs have been identified. CircRNAs modulate various bioprocesses, such as gene expression, cell proliferation, survival and mobility [6]. Additionally, growing evidence indicates that the abnormal circRNA expression was implicated in the progression of various cancers [7, 8]. For example, circC3P1 inhibits hepatic carcinoma through the microRNA (miR)-4641/PCK1 signal [9], circ-ZEB1.33 accelerates the growth of hepatic carcinoma by regulating miR-200a-3p/CDK6 [10], circHIPK3 promotes the progression of colorectal carcinoma via interacting with miR-7 [11], and circRNA ciRS-7 accelerates the progression of esophageal squamous cell carcinoma through miR-7/HOXB13 and miR-7/KLF4 [12,13]. Aberrant expression of circRNAs also has a close association with lung cancer. For instance, circMAN2B2 promotes the growth of lung cancer cells through regulating miR-1275/FOXK1 signal [14], circ_0062389 accelerates the proliferation and cell cycle progress of NSCLC via sponging miR-103a-3p [15], and circ_000984 promotes the progression of NSCLC through modulating the Wnt/β-catenin signal [16]. Nevertheless, the roles of circRNAs in NSCLC remain largely unknown. To investigate the role of circRNAs in NSCLC, we performed a high-throughput sequencing to profile the circRNAs expression in NSCLC tissues. Among the aberrantly expressed circRNAs, circ_0089823 (circBase ID: hsa_circ_0089823), a highly expressed circRNA in NSCLC tissues, caught our attention. Circ_0089823 is a circRNA located at chrX: 2871183-2873578 and its gene symbol is arylsulfatase E (ARSE). Whereas its role in NSCLC is not yet clear.

In this study, we investigated the role of circ_0089823 in NSCLC cells as well as its underlying mechanism. It will enrich our understanding on the role of circRNAs in lung cancer.

2 Materials and methods

2.1 Human lung cancer samples

Sixty-seven NSCLC samples and 18 adjacent non-cancer samples were acquired from NSCLC patients hospitalized in the Henan Provincial People's Hospital (Henan, China) from August 2015 to May 2016. Detailed information was shown in Table.S1. None of the patients received chemotherapy or radiotherapy before operation. Written informed consent was obtained from all patients. This study was in accordance with the Declaration of Helsinki and approved by the Ethics Committee of the Henan Provincial People's Hospital.

2.2 CircRNA high-throughput sequencing

Ten pairs of NSCLC samples and adjacent non-cancer samples were used for high-throughput sequencing. RNA was extracted and then 1% agarose gels were used to check the RNA degradation and contamination. A NanoPhotometer spectrophotometer (IMPLEN, Westlake Village, CA, USA) was used to check the RNA purity. A RNA Nano6000 assay kit of the Bioanalyzer 2100 system (Agilent Technologies, Santa Clara, CA, USA) was used to evaluate the RNA integrity. A QUBIT RNA assay kit in Qubit 2.0 Flurometer (Life Technologies, Carlsbad, CA, USA) was used to measure the RNA concentration. An epicenter ribozero rRNA removal kit (Epicentre, Madison, MI, USA) was used to wipe off ribosomal RNA. Sequencing library was generated with a NEBNext ultra directional RNA library prep kit (New England Biolabs, Ipswich, MA, USA). Raw reads were normalized by TPM. DESeq R package 1.10.1 was used to analyze the circRNAs with differential expression (fold change$\geq$ 2.0, p-value$<$ 0.05). Thereafter, GOseq R package was used for the gene ontology (GO) enrichment analysis and KOBAS software was used for the kyoto encyclopedia of genes and genomes (KEGG) pathway enrichment analysis of these circRNAs.

2.3 Cell culture and transfection

Human bronchial epithelial cells (HBE) were obtained from FUHENG Biology (Shanghai, China). PLA-801D, NCI-H1299, HCC827, NCI-H1437 and NCI-H446 cells (Procell, Wuhan, China) were maintained in RPMI-1640 (Gibco, Grand Island, NY, USA) containing 10% fetal bovine serum (FBS) (Hyclone, Logan, UT, USA). A549 cells (Procell) were grown in Ham's F-12K medium (Procell) containing 10% FBS. HEK-293T cells (Zhongqiaoxinzhou, Shanghai, China) were maintained in DMEM (Gibco) containing 10% FBS. All cells were cultured in a humidified atmosphere with 5% CO_2 at 37°C.

For transfection, circ_0089823 siRNAs (si-circ_0089823) and their negative control (si-NC), circ_0089823 shRNA (sh-circ_0089823) and its negative control (sh-NC) were transfected into A549 cells, while circ_0089823 over-expression plasmid (OE-circ_0089823) and its negative control (vector) were transfected into PLA-801D cells using Lipofectamine 2000 Reagent (Invitrogen, Carlsbad, CA, USA) according to the protocol. Similarly, microRNA mimics, inhibitors and their negative controls (mimics NC and inhibitor NC) were transfected into A549 cell and PLA-801D cells using Lipofectamine 2000 Reagent. Cells transfected with sh-circ_0089823, sh-NC, OE-circ_0089823 or vector were selected with G418 (350–400 μg/ml; Solarbio, Beijing, China) to obtain stably transfected cell clones.

2.4 Quantitative real-time PCR (qPCR)

A total RNA extraction kit (BioTeke) was used to extract the RNA and M-MLV reverse transcriptase (TaKaRa Bio, Osaka, Japan) was used in cDNA synthesis according to the manufacturer's protocol. Thereafter, qPCR was carried out to assess the level of circ_0089823, miR-507, miR-557, miR-579-3p, miR-1287-5p, sex-determining region Y-box (SOX) 4 and ARSE using SYBR Green method. The primers used were listed in Table S2. The relative mRNA levels of circ_0089823, SOX4 and ARSE were normalized to β-actin, and the relative levels of microRNAs were normalized to U6 snRNA. $2^{-\Delta\Delta Ct}$ and $2^{-\Delta Ct}$ method was applied to quantify the level of RNA.

2.5 Characteristics of circ_0089823

For PCR amplification assay, a genomic DNA (gDNA) extraction kit (BioTeke) was used to extract gDNA. cDNA or gDNA were used as the templates to amplify circ_0089823 using divergent or convergent primers in supplemental Table S3. The products were subjected into agarose gel electrophoresis. For RNaseR digestion assay, the extracted RNA was treated with RNaseR (Geneseed, Guangzhou, China) and then reversely transcribed to cDNA using random primers. The levels of circ_0089823 and ARSE were detected by qPCR. For reverse transcription assay, the extracted RNA was reversely transcribed into cDNA using oligo$(dT)_{15}$ or random primers. Then the levels of circ_0089823 and ARSE were detected using qPCR.

2.6 RNA fluorescence in situ *hybridization (FISH)*

Circ_0089823 probes were obtained from GenePharma (Shanghai, China). FISH was performed with a FISH kit (GenePharma) according to the protocol. 4′,6-diamidino-2-phenylindole (DAPI) was used to stain the nucleus. Cell images were captured with a fluorescence microscope (OLUMPUS, Tokyo, Japan).

2.7 Cell counting kit-8 (CCK-8) assays

Cells seeded in 96-well plates (3×10^3) were cultured for indicated time (0, 12, 24, 48 and 72 h). Then CCK-8 solution (10 μl; Sigma, St.Louis, MO, USA) was added into cells. After maintaining at 37°C for additional 1

h, the absorbance at 450 nm was measured by a microplate reader (BIOTEK, Winooski, VT, USA).

2.8 Colony formation assays

Cells seeded in 6-well plates (500 cells/ well) were cultured for 2 weeks. After fixation with 4% paraformaldehyde, the cells were stained with Wright's-Giemsa assay reagent (KeyGen, Nanjing, China). Cell images were captured, and the number of visible colonies was counted.

2.9 Flow cytometry analysis

An apoptosis determination kit (Beyotime, Shanghai, China) was used to determine cell apoptosis. The cells were collected and stained with annexin V-fluorescein isothiocyanate (FITC) and propidium iodide (PI) according to the instruction. Thereafter, the cells were analyzed with flow cytometry (NovoCyte, San Diego, CA, USA). Cell cycle determination was conducted with a cell cycle determination kit (Beyotime). The cells were collected and incubated with RNaseA and PI according to the instruction. Then the cells were monitored with a flow cytometer.

2.10 Western blot

Proteins in NSCLC samples, tumor bodies and cells were extracted and the protein concentration was determined with a bicinchoninic acid protein assay kit (Beyotime). Equal amount of proteins was separated by sodium dodecyl sulfate-polyacrylamide gel electrophoresis and transferred onto polyvinylidene difluoride membranes (Thermo Fisher, Waltham, Massachusetts). Afterward, the membranes were blocked with 5% bovine serum albumin (Biosharp, Hefei, China) and then incubated at 4°C overnight with antibodies recognizing cyclinD (1:1000; Abclonal, Wuhan, China), cyclinE (1:1000; Proteintech, Wuhan, China), Bcl-2 (1:500; ABclonal), Bax (1:500; ABclonal), SOX4 (1:1000; Affinity, Changzhou, China) and β-actin (1:2000; Proteintech). After washing with tris-buffered saline with tween, the membranes were incubated at 37°C for 40 min with horseradish peroxidase-conjugated secondary antibodies (Proteintech). Finally, the membranes were visualized using a chemiluminescence detection system (7sea biotech, Shanghai, China). β-Actin served as the internal control.

2.11 Caspase-3 and caspase-9 activity determination

Caspase-3 and caspase-9 activities were detected with a caspase-3 activation detection kit (Beyotime) and a caspase-9 activity detection kit (Solarbio) according to the instruction.

2.12 AGO2-RNA immunoprecipitation (RIP)

AGO2-RIP assay was performed with an EZ-Magna Kit (Millipore, Bedford, MA, USA). Briefly, cells were lysed with RIP lysis buffer. After centrifugation, the cell lysates were incubated with magnetic beads pre-coated with human AGO2 antibody in RIP buffer. Afterward, the proteins were digested with proteinase K and the RNA was then purified. Thereafter, PCR was performed to amplify circ_0089823, miR-579-3p, miR-1287-5p, miR-507 and miR-557. Immunoglobulin G (IgG) served as a negative control.

2.13 Luciferase reporter assay

To demonstrate the interaction between circ_0089823 or SOX4 and miR-507, miR-557, miR-579-3p or miR-1287-5p, wild-type (WT) or mutant (MUT) binding sequences for circ_0089823 or SOX4 were subcloned into pmirGLO vectors (GeneScript, Nanjing, China). The plasmids mentioned and microRNA mimics or mimics NC above were co-transfected into HEK-293T cells. The luciferase activity was determined with a luciferase activity assay kit (Promega, Madison, WI, USA) according to the protocol.

2.14 In vivo *xenograft mouse models*

4-week-old male BALB/c nude mice (Huafukang Bioscience, Beijing, China) were fed in a standard environment (12 h-light/dark cycles; 21-23°C; humidity 45-55%). A xenograft model was established by subcutaneously injecting stably transfected cells into the flanks of nude mice (1×10^7 /200 μl; n=6 for each group). Twenty-one days later, the mice were sacrificed and the xenografts were harvested for subsequent experiments. All animal experimental protocols were in accordance with the Guide for Care and Use of Laboratory Animals and approved by the Ethics Committee of Henan Provincial People's Hospital.

2.15 Immunofluorescence

Paraffin-embedded xenografts were cut into slices (5 μm). After deparaffinization, rehydration and antigen retrieval, the slices were blocked with goat serum (Solarbio). Thereafter, the slices were incubated with Ki-67 antibody (ABclonal) at 4°C overnight, followed by incubating with Cy3-conjugated secondary antibody (Beyotime). The slices were observed using a fluorescence microscope (OLUMPUS).

2.16 Terminal deoxynucleotidyl transferase-mediated dUTP nick end labelling (TUNEL)

An *in situ* cell death determination kit (Roche, Penzberg, Germany) was used in TUNEL assay. After deparaffinization, rehydration, and permeabilization, the slices were blocked with 3% hydrogen peroxide and then incubated with TUNEL reaction solution at 37°C for 60 min, followed by Converter-POD solution at 37°C for 30 min. Afterward, the slices were developed with a DAB substrate kit (Solarbio), counterstained with hematoxylin and observed with a microscope (OLUMPUS).

2.17 Statistical analysis

GraphPad Prism 8 (GraphPad, San Diego, CA) was used for data analysis with one-way analysis of variance or Student's *t* test. The relationship between circ_0089823 and pathology characters was analyzed using chi-square test. The area under the curve (AUC) was calculated based on the receiver operating characteristic (ROC) curve. Data are presented as mean ± standard deviation (SD). $P < 0.05$ was considered to be significantly differential.

3 Results

3.1 CircRNAs profiles in NSCLC

High-throughput sequencing was carried out to detect the expression of circRNAs in 10 NSCLC samples and paired adjacent non-cancer samples. A total of 29075 circRNAs were identified (Fig. 1A). In NSCLC samples, there were 183 circRNAs up-regulated and 428 circRNAs down-regulated (fold change≥ 2, *P*value < 0.05) (Fig. 1B). Additionally, based on the circRNA profile, a hierarchical clustering analysis was performed to visualize the expression pattern of these circRNAs (Fig. 1C). The top 10 up-regulated and top 10 down-regulated circRNAs were listed in Table 1. Afterward, these circRNAs were annotated and subjected to GO analysis (Fig. 1D). The majority of biological process (BP) was "anatomical structure development" (202/472), "single-organism developmental process" (191/472) and "cellular developmental process" (162/472). The majority of cellular component (CC)

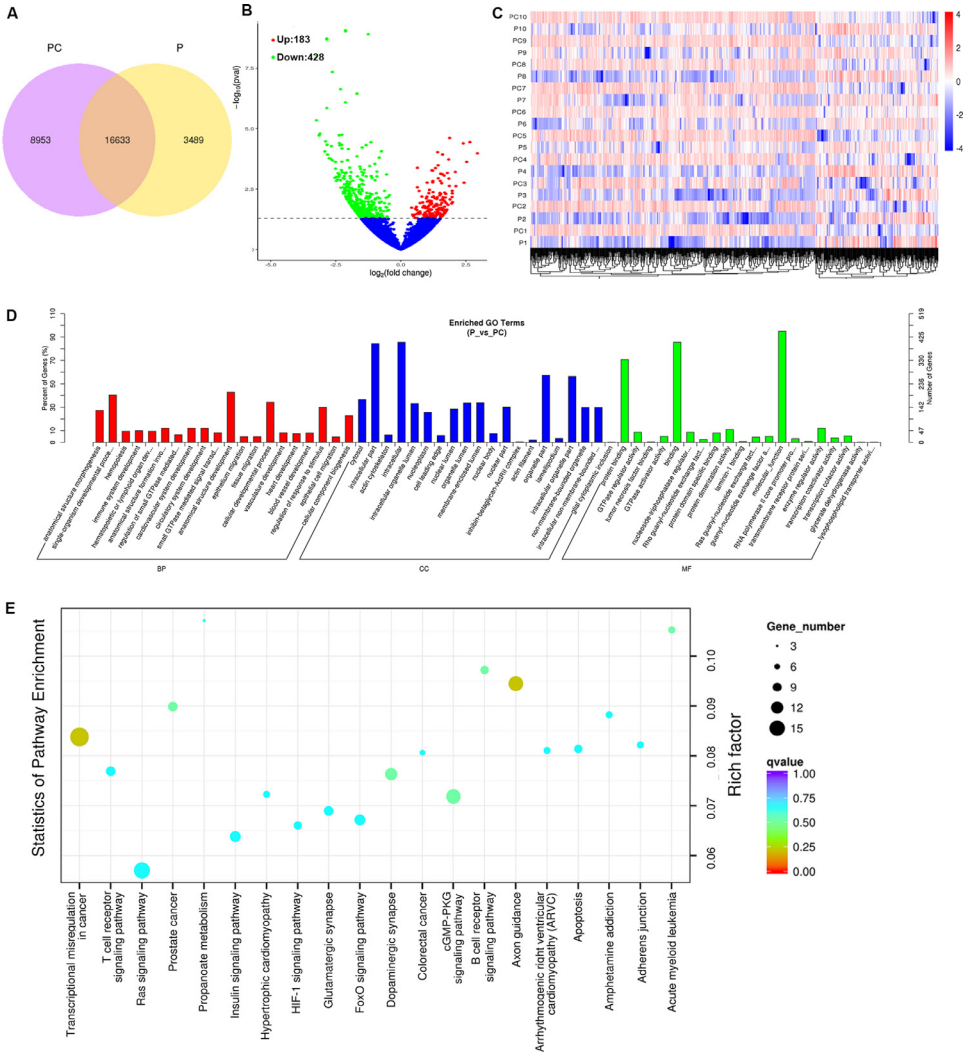

Fig. 1. CircRNA expression profile in NSCLC samples. The circRNAs expression profile in the NSCLC samples and adjacent non-cancer samples was determined using high-throughput sequencing. There were a total of 29075 circRNAs identified (A). Among them, 183 circRNAs were up-regulated and 428 circRNAs were down-regulated in NSCLC samples (B). CircRNAs with abnormal expression were subjected to classification analysis (C), GO analysis (D) and KEGG analysis (E).

was "intracellular" (404/472), "intracellular part" (298/472) and "organelle part" (271/472). "Molecular function" (448/472), "binding" (404/472) and "protein binding" (334/472) were the majority of molecular function (MF). In addition, KEGG enrichment analysis was performed and the top 20 items were shown in Fig. 1E. Among these items, the Ras, HIF-1, FoxO, and cGMP-PKG pathways have close relationship with the development of cancers.

3.2 Circ_0089823 is highly expressed in NSCLC samples

According to the results of high-throughput sequencing, circ_0089823 was highly expressed in NSCLC samples. However, its role remains unclear. We are interested in the role of circ_0089823 in NSCLC. Circ_0089823 is located at chrX: 2871183-2873578 (Fig. 2A). To explore the characteristics of circ_0089823, divergent primers and convergent primers were designed to amplify circ_0089823. As shown in Fig. 2B, using gDNA as the template, there were amplification products using convergent primers, but not the divergent primers. However, when the template was changed to cDNA, there were amplification products using both convergent primers and divergent primers (Fig. 2B). Furthermore, circ_0089823 can be amplified with random primers, but not oligo(dT) primers (Fig. 2C). In addition, RNaseR treatment assay showed that circ_0089823 was more stable than linear ARES. (Fig. 2D). These results revealed that circ_0089823 was a stable circular RNA. RNA FISH showed that circ_0089823 was predominantly located in the cytoplasm (Fig. 2E).

The level of circ_0089823 in 18 NSCLC samples and paired adjacent non-cancer samples was detected by qPCR. Compared with the adjacent non-cancer samples, NSCLC samples showed a higher level of circ_0089823 (Fig. 3A). Its level was able to differentiate NSCLC tissues from normal non-cancer tissues, with an AUC of 0.9537 ($P < 0.001$; 95% confidence interval: 0.8926–1.000) (Fig. 3B). In addition, the circ_0089823 level was determined in an enlarged dataset (n=67) and the relationship between circ_0089823 and pathology characters of NSCLC patients was analyzed (Table 2). The results showed that more male patients tended to a high circ_0089823. Interestingly, nearly all squamous cell carcinoma tended to a high circ_0089823. Moreover, the level of circ_0089823 is also associated with the TNM stage of NSCLS. More NSCLS with low invasion or no lymph node metastasis tended to a low circ_0089823. Nearly all NSCLS

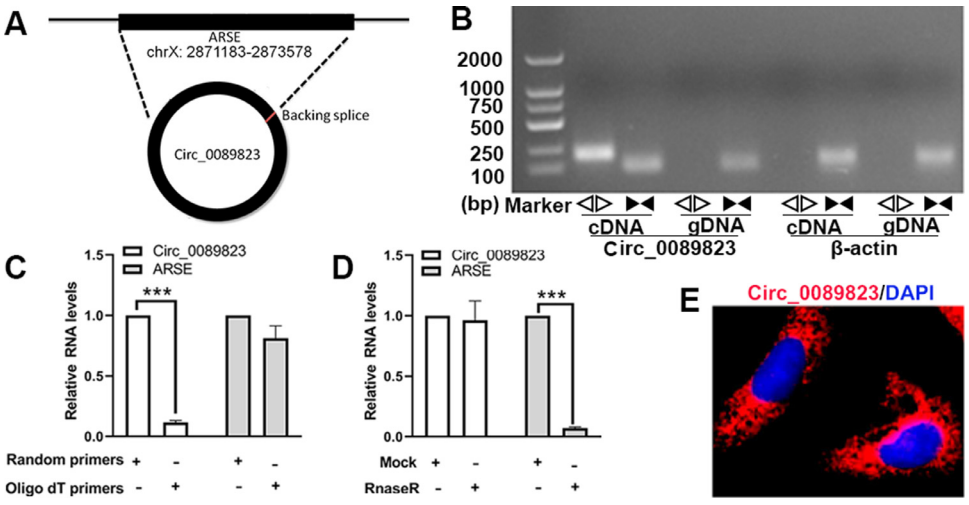

Fig. 2. Characteristics of circ_0089823. (A) Ideogram of circ_0089823. (B) PCR product amplified with convergent primers and divergent primers. (C) Amplification of circ_0089823 and ARSE with random primers or oligo dT primers. (D) Amplification of circ_0089823 and ARSE after RnaseR treatment. (E) Distribution of circ_0089823 identified by RNA fluorescence *in situ* hybridization. The results are presented as mean± SD. *** $P < 0.001$.

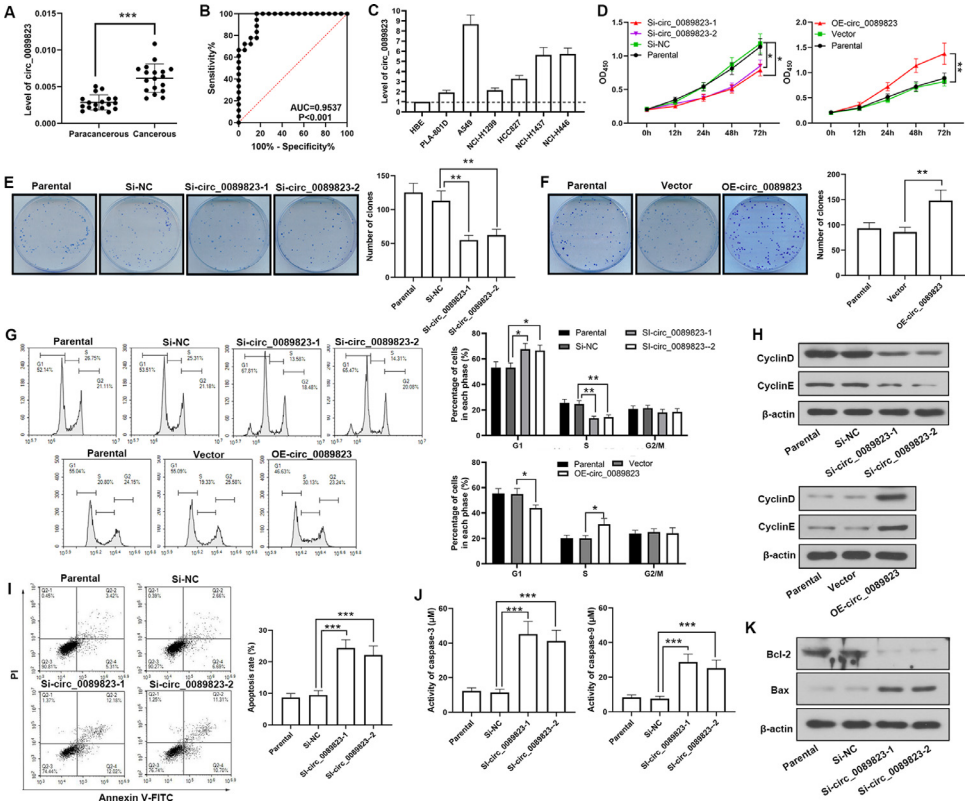

Fig. 3. Circ_0089823 promotes NSCLC cell growth *in vitro.* (A) The level of circ_0089823 in NSCLC and adjacent non-cancer samples was detected by qPCR. (B) The ROC curve for circ_0089823 to differentiate NSCLC tissues from non-cancer tissues. (C) The level of circ_0089823 in NSCLC cell lines was detected by qPCR. (D) After transfection with circ_0089823 siRNAs or its over-expression plasmid, CCK-8 assay was conducted to evaluate the proliferation of NSCLC cells. (E-F) Colony formation assay was carried out after transfection. (G) Cell cycle was determined by flow cytometry after transfection. (H) After transfection, western blot was conducted to determine the levels of cyclinD and cyclinE. (I) After transfection, apoptosis was determined by flow cytometry. (J) The activities of caspase-3 and caspase-9 after transfection. (K) The levels of Bcl-2 and Bax were determined by western blot. The results were presented as mean ± SD. * $P < 0.05$, ** $P < 0.01$, *** $P < 0.001$.

Table 1

Top 10 up-regulated circRNAs and top 10 down-regulated circRNAs.

CircRNAs	Up- or down-regulation	Log_2 Fold change	*P* value
Novel_circ_0009428	Up	2.9455	0.000104
Hsa_circ_0001387	Up	2.6551	0.000036
Hsa_circ_0003074	Up	2.5323	0.000237
Hsa_circ_0089823	Up	2.4308	0.001720
Hsa_circ_0006922	Up	2.4012	0.000040
Hsa_circ_0049282	Up	2.1176	0.002376
Novel_circ_0026406	Up	2.0943	0.000620
Hsa_circ_0048259	Up	1.9885	0.010976
Novel_circ_0008518	Up	1.9782	0.004694
Novel_circ_0006906	Up	1.9764	0.003724
Novel_circ_0030300	Down	-3.2418	0.000005
Novel_circ_0029532	Down	-3.1404	0.000019
Novel_circ_0020451	Down	-3.1095	0.000016
Novel_circ_0021669	Down	-2.9198	0.000088
Novel_circ_0011120	Down	-2.8915	0.000033
Hsa_circ_0008386	Down	-2.8446	0.000001
Hsa_circ_0008158	Down	-2.8365	0.000046
Hsa_circ_0000169	Down	-2.8183	0.000118
Novel_circ_0040982	Down	-2.7528	0.000168
Novel_circ_0009279	Down	-2.6951	0.000176

Table 2

The relationship between circ_0089823 and pathology characters of NSCLC patients.

Characteristics	Patients (n = 67)	Expression of circ_0089823 High (n = 33)	2 Low (n = 34)	χ^2	*P* value
Gender					
Male	28	20	8	9.46	**0.0021** **
Female	39	13	26		
Age (year)					
<60	30	13	17	0.76	0.3828
≥60	37	20	17		
Tumor size (cm)					
<3	44	12	32	24.78	***P* < 0.001****
≥3	23	21	2		
Pathological type					
Adenocarcinoma	57	23	34	12.11	**0.0005** ***
Squamous cell carcinoma	10	10	0		
Tumor invasion					
T1	49	15	34	25.36	***P* < 0.001** ***
T2+T3+T4	18	18	0		
Lymph node metastasis					
N0	56	22	34	13.56	**0.0002** ***
N1	11	11	0		
Distant metastasis					
M0	65	31	34	2.12	0.1450
M1	2	2	0		
TNM stage					
I	53	19	34	18.23	***P* < 0.001** ***
II+III+IV	14	14	0		
Smoking history					
Yes	19	17	2	17.16	***P* < 0.001** ***
No	48	16	32		

with higher TNM stage, such as T2-T4 invasion, lymph node metastasis or distant metastasis showed a high circ_0089823. On the other hand, the circ_0089823 was also associated with smoking. More NSCLC patients with smoking history intend to a high circ_0089823.

3.3 Circ_0089823 reinforces the growth of NSCLC in vitro

On the other hand, the level of circ_0089823 in lung cancer cell lines was higher than the normal cell line HBE (Fig. 3C). To explore the function of circ_0089823, over-expression plasmid and siRNAs for

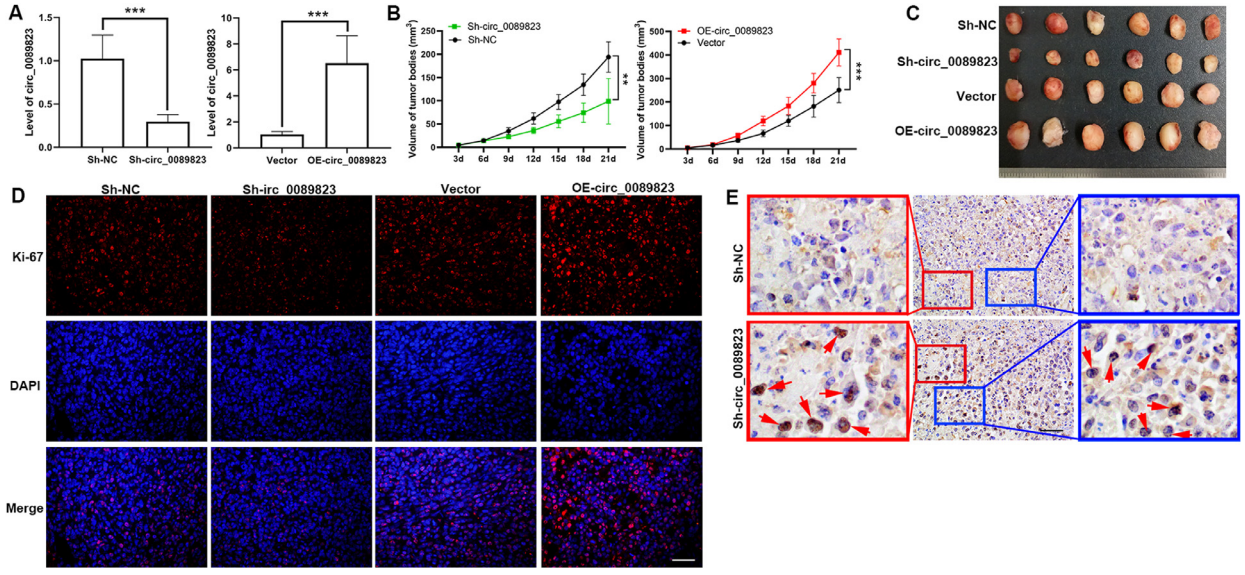

Fig. 4. Circ_0089823 promotes NSCLC xenograft growth *in vivo.* Circ_0089823 silenced A549 cells and circ_0089823 over-expressed PLA-801D were subcutaneously injected into the flanks of nude mice. (A) The level of circ_0089823 in xenografts was detected by qPCR. (B) The growth of xenografts. (C) Images of xenografts. (D) The level of Ki-67 in xenografts was detected by immunofluorescence staining. (E) TUNEL staining was conducted to detect apoptosis in xenografts. Arrows indicated TUNEL-positive cells. The results were presented as mean± SD. ** $P < 0.01$, *** $P < 0.001$.

circ_0089823 were employed in this study, and their transfection efficiencies were measured using qPCR (Fig. S1). In cells transfected with circ_0089823 siRNAs, the proliferation of NSCLC cells was decelerated, while in cells with circ_0089823 over-expression, the proliferation of NSCLC cells was accelerated (Fig. 3D). Consistently, the colony number was decreased in circ_0089823 silenced cells, whereas, increased in circ_0089823 over-expressed cells (Fig. 3E and F). The function of circ_0089823 on cell cycle was also evaluated. In circ_0089823 silenced cells, the percentage of G1 phase was risen and the percentage of S phage was declined, while in circ_0089823 over-expressed cells, the percentage of G1 phase was declined, while the percentage of S phage was risen (Fig. 3G). In addition, the levels of cyclinD and cyclinE were decreased in circ_0089823 silenced cells, but increased in circ_0089823 over-expressed cells (Fig. 3H). Besides, in cells transfected with circ_0089823 siRNAs, the percentage of apoptotic cells was elevated (Fig. 3I), with increased caspase-3 and caspase-9 activities (Fig. 3J), increased Bax level and decreased Bcl-2 level (Fig. 3K). These results demonstrate that circ_0089823 promotes the proliferation of NSCLC cells, accelerates cell cycle and represses apoptosis.

3.4 Circ_0089823 promotes the growth of NSCLC cells in vivo

The function of circ_0089823 on NSCLC cell growth was also determined *in vivo*. First, the efficiencies of circ_0089823 silencing and over-expression in xenografts were detected by qPCR (Fig. 4A). Xenografts with circ_0089823 silencing grew more slowly, while xenografts with circ_0089823 over-expression grew more quickly than the negative control (Fig. 4B). Consistently, the volume of xenografts with circ_0089823 silencing was smaller, while the volume of xenografts with circ_0089823 over-expression was larger than the negative control (Fig. 4C). In addition, xenograft growth was also evaluated by immunofluorescence staining with Ki-67, a biomarker for cell proliferation. The Ki-67 signal was lower in xenografts with circ_0089823 silencing, while higher in xenografts with circ_0089823 over-expression than the negative control (Fig. 4D). Otherwise, there were more TUNEL-positive cells in xenografts with circ_0089823 silencing than the negative control (Fig. 4E), indicating increased apoptosis. These data elucidate that circ_0089823 promotes the growth of NSCLC *in vivo*.

3.5 Circ_0089823 and SOX4 are targeted by miR-507, miR-557, miR-579-3p, and miR-1287-5p

Bioinformatics website Circular RNA Interactome (https://circinteractome.nia.nih.gov/) was used to predict microRNAs which could bind with circ_0089823 (shown in Fig. 5A). Among them, we are interested in miR-507, miR-557, miR-579-3p and miR-1287-5p, which were lowly expressed in NSCLC samples (Fig. 5B). Additionally, following the assessment of transfection efficiencies of mimics and inhibitors of these microRNAs by qPCR (Fig. S2), the function of these microRNAs on NSCLC cell proliferation was assessed by CCK-8. Up-regulation of these 4 microRNAs repressed, while down-regulation of these microRNAs accelerated NSCLC cell proliferation (Fig. 5C).

To verify the predicted binding between circ_0089823 and miR-507, miR-557, miR-579-3p, miR-1287-5p, an AGO2-RIP assay was conducted. In the AGO2 immunoprecipitate, there were both circ_0089823 and miR-507, miR-557, miR-579-3p, miR-1287-5p (Fig. 5D). In addition, luciferase reporter assay was conducted. In cells co-transfected with circ_0089823 WT and mimics of these 4 microRNAs, the relative luciferase activity was significantly decreased compared with cells co-transfected with circ_0089823 WT and mimics NC, while these microRNAs failed to decrease the relative luciferase activity in circ_0089823 MUT group (Fig. 5E), indicating that circ_0089823 can be bound by these 4 microRNAs. Subsequently, the level of circ_0089823 was decreased by mimics of these 4 microRNAs, and increased by inhibitors of these microRNAs (Fig. 5F), indicating that circ_0089823 is targeted by these 4 microRNAs.

In the 3′ untranslated region (UTR) of SOX4, there were also predicted binding sites for miR-507, miR-557, miR-579-3p and miR-1287-5p. A luciferase reporter assay was conducted to verify the potential bond between SOX4 and these 4 microRNAs. Mimics of these 4 microRNAs decreased the luciferase activity of wild-type SOX4, whereas, failed to affect the luciferase activity of mutant SOX4 (Fig. 6A-D). In addition, the mRNA and protein levels of SOX4 were decreased by mimics of these 4 microRNAs, and increased by inhibitors of these microRNAs (Fig. 6E-L). These results demonstrate that SOX4 is bound and regulated by these 4 microRNAs.

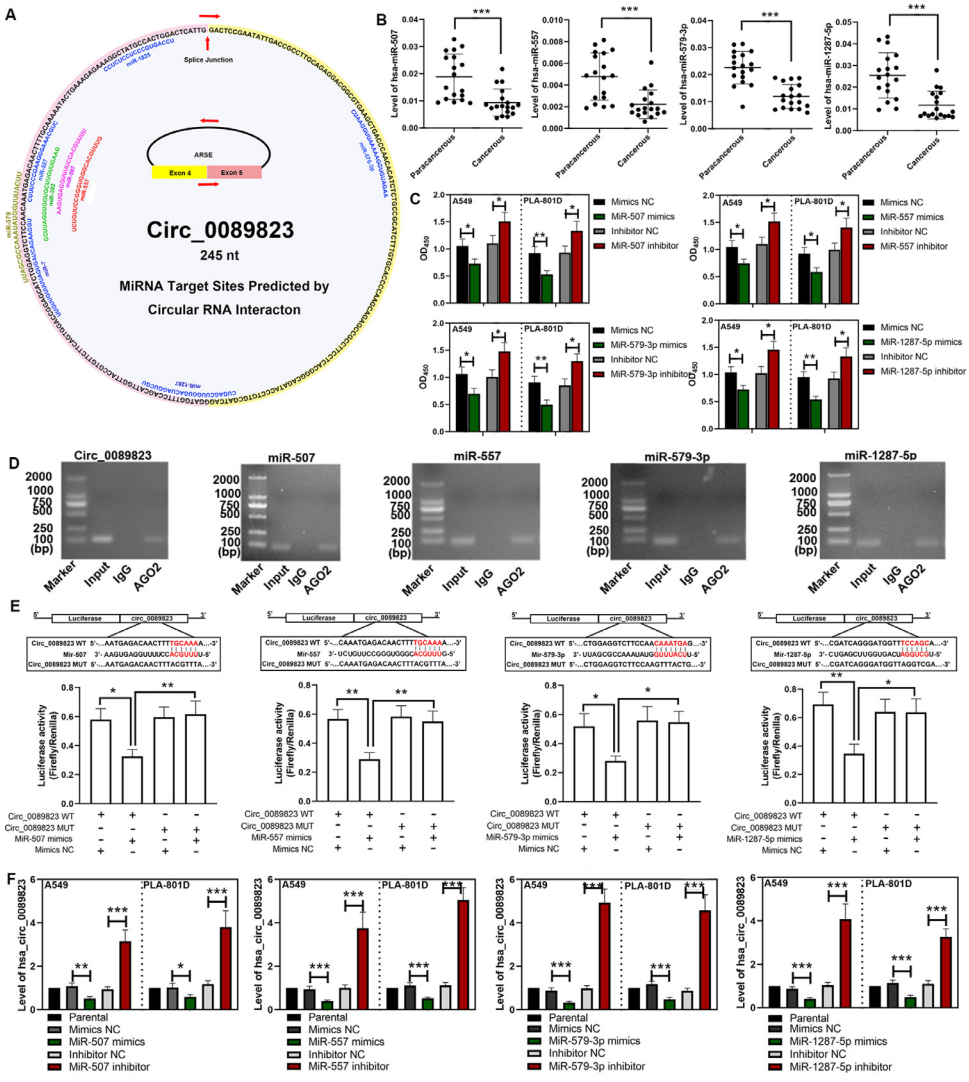

Fig. 5. Circ_0089823 is targeted by miR-507, miR-557, miR-579-3p, and miR-1287-5p. (A) Ideogram for microRNA binding sites in circ_0089823. (B) The levels of miR-507, miR-557, miR-579-3p and miR-1287-5p in NSCLC samples were detected by qPCR. (C) After transfection with mimics or inhibitors of these microRNAs, the proliferation of NSCLC cells was assessed by CCK-8 assay. (D) The bond between these 4 microRNAs and circ_0089823 was confirmed by AGO2-RIP. (E) The direct binding between circ_0089823 and these 4 microRNAs were verified by luciferase reporter assay. (F) After transfection with mimics or inhibitors of these 4 microRNAs, the level of circ_0089823 was detected by qPCR. The results were presented as mean± SD. * $P < 0.05$, ** $P < 0.01$, *** $P < 0.001$.

3.6 Circ_0089823 accelerates NSCLC cell growth through up-regulating SOX4

The level of SOX4 in NSCLC samples was higher than in the adjacent non-cancer tissues (Fig. 7A), which was similar to that of circ_0089823. Besides, circ_0089823 silencing decreased the mRNA and protein levels of SOX4, whereas, circ_0089823 over-expression increased SOX4 *in vitro* (Fig. 7B and C). Moreover, the level of SOX4 *in vivo* was also decreased by circ_0089823 shRNA and increased by circ_0089823 over-expression (Fig. 7D and E). These data showed that circ_0089823 positively regulated that expression of SOX4. Furthermore, we explored whether circ_0089823 performed its role through the regulation of SOX4. The efficiencies of SOX4 siRNA and SOX4 over-expression plasmid were determined by qPCR (Fig.S3). Over-expressing SOX4 increased the level of SOX4 which was decreased by circ_0089823 silencing and SOX4 silencing decreased the level of SOX4 which was increased by circ_0089823 over-expression (Fig. 7F). Interestingly, silencing SOX4 repressed the NSCLC cell proliferation which was promoted by circ_0089823 over-expression (Fig. 7G). Consistently, SOX4 over-expression abolished the effect of circ_0089823 silencing on the proliferation and apoptosis of NSCLC cells (Fig. 7G,H). These results demonstrate that circ_0089823 promotes the growth of NSCLC through up-regulating SOX4. Thus we hypothesis that circ_0089823 may regulate the expression of SOX4 via sponging miR-507, miR-557, miR-579-3p and miR-1287-5p, thus accelerating the growth of NSCLC cells (Fig. 8).

4 Discussion

In recent years, circRNAs have attracted more and more attention of researchers. We profiled the circRNA expression in NSCLC samples through high-throughput sequencing. There were 183 up-regulated circRNAs and 428 down-regulated circRNAs. They may be involved in the progression of NSCLC. In this study, we explored the role of circ_0089823, a highly

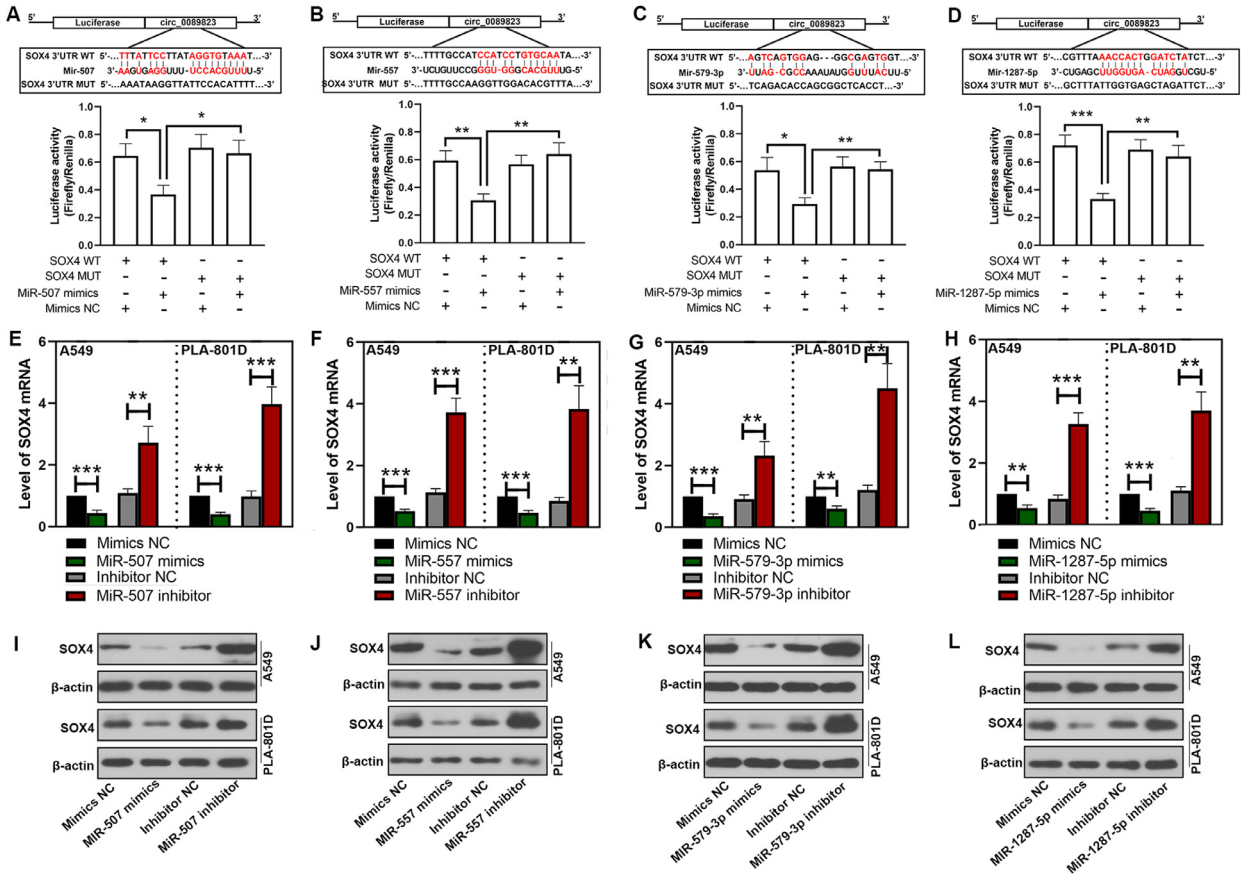

Fig. 6. SOX4 is targeted by miR-507, miR-557, miR-579-3p and miR-1287-5p. (A-D) The binding between SOX4 and these 4 microRNAs was verified by luciferase reporter assay. (E-H) After transfection with mimics or inhibitor of these 4 microRNAs, the level of SOX4 was detected by qPCR. (I-L) The level of SOX4 in NSCLC cells was determined by western blot after transfection. The results were presented as mean± SD. * $P < 0.05$, ** $P < 0.01$, *** $P < 0.001$.

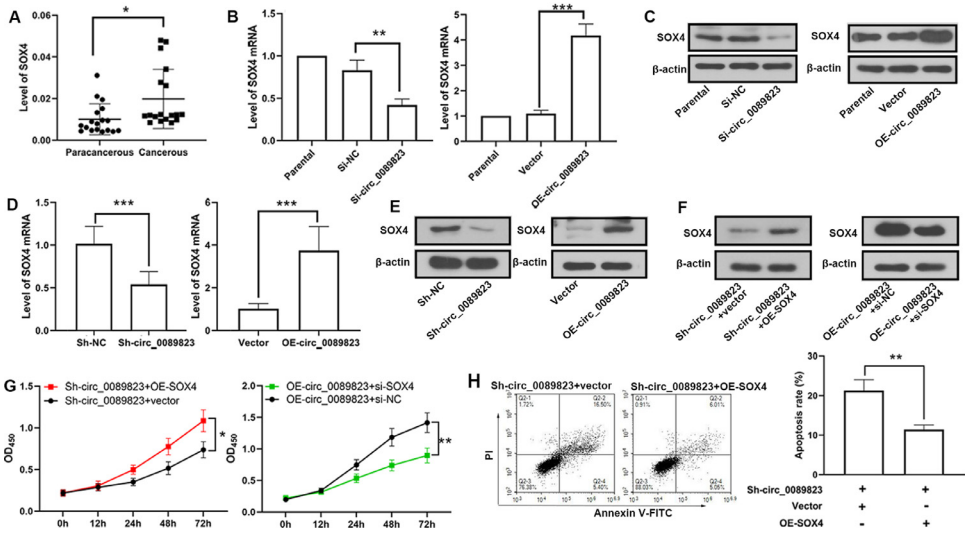

Fig. 7. Circ_0089823 promotes NSCLC cell growth through up-regulating SOX4. (A) The level of SOX4 in NSCLC samples and adjacent non-cancer samples was detected by qPCR. (B) The level of SOX4 in circ_0089823 silenced cells and circ_0089823 over-expressed cells were detected by qPCR. (C) Western blot was conducted to determine the SOX4 level in circ_0089823 silenced cells and circ_0089823 over-expression cells. (D-E) The level of SOX4 in xenografts was detected by qPCR and western blot. (F) Western blot was conducted to determine the level of SOX4 in cells co-transfected with circ_0089823 shRNA plus SOX4 OE or circ-0089823 OE plus SOX4 siRNA. (G) Proliferation of cells was evaluated by CCK-8 after co-transfection. (H) Apoptosis was detected by flow cytometry after co-transfection. The results were presented as mean± SD. * $P < 0.05$, ** $P < 0.01$, *** $P < 0.001$.

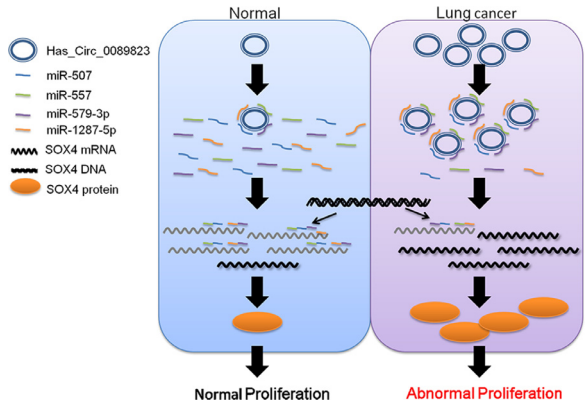

Fig. 8. Ideograph of hypothesis that circ_0089823 promotes NSCLC growth through up-regulating SOX4 via sponging miR-507, miR-557, miR-579-3p, and miR-1287-5p.

expressed circRNA in NSCLC. Besides gender and tumor size, the level of circ_0089823 is related to pathological type, TNM stage and smoking history of NSCLC patients, indicating a critical role of circ_0089823 in NSCLC. Circ_0089823 was declared to accelerate NSCLC cell growth through up-regulating SOX4 via sponging microRNAs. This study will enrich our understanding on the role of circRNAs in lung carcinoma. It may contribute to novel therapeutic strategies for NSCLC.

Growing evidence indicates the significant roles of circRNAs in NSCLC. In our study, we identified circ_0089823 as a highly expressed circRNA in NSCLC samples, which was consistent with the results of high-throughput sequencing. We confirmed that circ_0089823 was mainly located in the cytoplasm. It had a loop structure lacking of a polyA tail which made it more stable than linear ARSE. In addition, silencing circ_0089823 suppressed the proliferation and induced cell cycle arrest and apoptosis in NSCLC cells, while over-expressing circ_0089823 resulted in opposite phenomenon. Consistent with our *in vitro* consequences, circ_0089823 also promoted xenograft growth *in vivo*. It is indicated that circ_0089823 may participate in cell growth control and contribute to NSCLC carcinogenesis. This study prompts us that circ_0089823 has the potential to become a candidate target for NSCLC treatment.

MicroRNAs are a class of endogenous non-coding RNAs. They post-transcriptionally regulate the expression of target genes via binding to the 3′UTR of target genes [17]. Emerging evidence reveals that microRNAs play important roles in cellular processes and are implicated in diverse human diseases, including cancers [18]. For instance, miR-507 inhibits the malignant behaviors of NSCLC and breast cancer through targeting zinc finger E-box binding homeobox 2 and Fms-related tyrosine kinase-1 [19,20], miR-557 served as a tumor suppressor in pancreatic and lung cancer via targeting lymphocyte enhancement factor 1 and phosphoinositide 3-kinase CB [21,22], miR-579-3p represses the proliferation and metastasis of small cell lung cancer cells [23] and miR-1287-5p suppresses the growth of breast and hepatocellular carcinoma [24,25]. MicroRNAs can also bind with non-coding RNAs, such as lncRNAs and circRNAs. In recent years, accumulating studies identified that circRNAs may play their roles through sponging microRNAs. Owing to online prediction, there are microRNA response elements for miR-507, miR-557, miR-579-3p and miR-1287-5p in circ_0089823. We verified that circ_0089823 can bind directly with these 4 microRNAs. Moreover, the low levels and proliferation-repression action of these 4 microRNAs were opposite to the level and function of circ_0089823. These results prompt us that circ_0089823 may perform its function in NSCLC cells through sponging these microRNAs. On the other hand, in circ_0089823, there are microRNA response elements for other microRNAs which may mediate the function of circ_0089823.

SOX4, one of the transcription factor SOX family, is implicated in normal development [26]. It binds with the DNA minor groove, resulting in chromatin architecture alterations and downstream gene expression changes. Notably, accumulating evidence reveals that SOX4 is abnormally expressed in multiple cancers and associated with tumor progression [27–32]. Various key signaling pathways, including the β-catenin [33] and NF-κB [34] signals, are modulated by SOX4. Bionformatics analysis showed that in the 3′UTR of SOX4, there were also microRNA response elements for miR-507, miR-557, miR-579-3p and miR-1287-5p. As predicted, we confirmed that SOX4 was directly targeted by these 4 microRNAs. SOX4 is highly expressed in NSCLC tissues and has a positive correlation with its clinical characteristics [35]. The level of SOX4 may also serve as a potential biomarker for the malignant status or poor prognosis of NSCLC patients [35]. Moreover, SOX4 silencing was reported to inhibit the growth of lung cancer cells [36,37], indicating an oncogene-like role of SOX4 in modulating the malignant phenotypes of lung cancer. Thus, we conclude that SOX4 may mediate the function of these 4 microRNAs.

Bioinformatic analysis showed that there were microRNA response elements for the same microRNAs in both circ_0089823 and the 3′UTR of SOX4. Interestingly, we found that the expression of SOX4 was positively regulated by circ_0089823. Owing to that circRNAs can perform their functions as a sponge of microRNAs, we hypothesized that circ_0089823 may sponge these microRNAs, resulting in positively regulation of SOX4, thus accelerating the NSCLC cell growth. More importantly, silencing SOX4 abrogated the function of circ_0089823, confirming that circ_0089823 facilitates NSCLC cell growth through up-regulating the expression of SOX4 via sponging microRNAs. SOX4 is also implicated in the epithelial-to-mesenchymal transition of NSCLC cells, which contributes to tumor metastasis [36,38]. Through regulating SOX4, circ_0089823 may also participate in the regulation of NSCLC metastasis, which may be further investigated in our future study. Additionally, circRNAs, lncRNAs and target genes of microRNAs constitute a huge network using microRNAs as the nodes. The results of our study unveiled part of this network. Other target genes of these microRNAs may also contribute to the function of circ_00989823.

In conclusion, we revealed that circ_0089823 was highly expressed in NSCLC samples and accelerated NSCLC cell growth through up-regulating SOX4 via sponging miR-507, miR-557, miR-579-3p, and miR-1287-5p. Circ_0089823, which exerts a cancer-promoting role in NSCLC, may serve as a potential therapeutic target for the treatment of NSCLC.

Supplementary materials

Supplementary material associated with this article can be found, in the online version, at doi:10.1016/j.neo.2021.06.011.

References

[1] Bray F, Ferlay J, Soerjomataram I, Siegel RL, Torre LA, Jemal A. Global cancer statistics 2018: GLOBOCAN estimates of incidence and mortality worldwide for 36 cancers in 185 countries. *CA Cancer J Clin* 2018;**68**:394–424.

[2] Chen Z, Fillmore CM, Hammerman PS, Kim CF, Wong KK. Non-small-cell lung cancers: a heterogeneous set of diseases. *Nat Rev Cancer* 2014;**14**:535–46.

[3] Gupta GP, Massague J. Cancer metastasis: building a framework. *Cell* 2006;**127**:679–95.

[4] Li X, Yang L, Chen LL. The biogenesis, functions, and challenges of circular RNAs. *Mol Cell* 2018;**71**:428–42.

[5] Kristensen LS, Andersen MS, Stagsted LVW, Ebbesen KK, Hansen TB, Kjems J. The biogenesis, biology and characterization of circular RNAs. *Nat Rev Genet* 2019;**20**:675–91.

[6] Li J, Yang J, Zhou P, Le Y, Zhou C, Wang S, Xu D, Lin HK, Gong Z. Circular RNAs in cancer: novel insights into origins, properties, functions and implications. *Am J Cancer Res* 2015;**5**:472–80.

[7] Dong Y, He D, Peng Z, Peng W, Shi W, Wang J, Li B, Zhang C, Duan C. Circular RNAs in cancer: an emerging key player. *J Hematol Oncol* 2017;**10**:2.

[8] Kristensen LS, Hansen TB, Veno MT, Kjems J. Circular RNAs in cancer: opportunities and challenges in the field. *Oncogene* 2018;**37**:555–65.

[9] Zhong L, Wang Y, Cheng Y, Wang W, Lu B, Zhu L, Ma Y. Circular RNA circC3P1 suppresses hepatocellular carcinoma growth and metastasis through miR-4641/PCK1 pathway. *Biochem Biophys Res Commun* 2018;**499**:1044–9.

[10] Gong Y, Mao J, Wu D, Wang X, Li L, Zhu L, Song R. Circ-ZEB1.33 promotes the proliferation of human HCC by sponging miR-200a-3p and upregulating CDK6. *Cancer Cell Int* 2018;**18**:116.

[11] Zeng K, Chen X, Xu M, Liu X, Hu X, Xu T, Sun H, Pan Y, He B, Wang S. CircHIPK3 promotes colorectal cancer growth and metastasis by sponging miR-7. *Cell Death Dis* 2018;**9**:417.

[12] Li RC, Ke S, Meng FK, Lu J, Zou XJ, He ZG, Wang WF, Fang MH. CiRS-7 promotes growth and metastasis of esophageal squamous cell carcinoma via regulation of miR-7/HOXB13. *Cell Death Dis* 2018;**9**:838.

[13] Huang H, Wei L, Qin T, Yang N, Li Z, Xu Z. Circular RNA ciRS-7 triggers the migration and invasion of esophageal squamous cell carcinoma via miR-7/KLF4 and NF-kappaB signals. *Cancer Biol Ther* 2019;**20**:73–80.

[14] Ma X, Yang X, Bao W, Li S, Liang S, Sun Y, Zhao Y, Wang J, Zhao C. Circular RNA circMAN2B2 facilitates lung cancer cell proliferation and invasion via miR-1275/FOXK1 axis. *Biochem Biophys Res Commun* 2018;**498**:1009–15.

[15] She Y, Han Y, Zhou G, Jia F, Yang T, Shen Z. hsa_circ_0062389 promotes the progression of non-small cell lung cancer by sponging miR-103a-3p to mediate CCNE1 expression. *Cancer Genet* 2020;**241**:12–19.

[16] Li XY, Liu YR, Zhou JH, Li W, Guo HH, Ma HP. Enhanced expression of circular RNA hsa_circ_000984 promotes cells proliferation and metastasis in non-small cell lung cancer by modulating Wnt/beta-catenin pathway. *Eur Rev Med Pharmacol Sci* 2019;**23**:3366–74.

[17] Saliminejad K, Khorram Khorshid HR, Soleymani Fard S, Ghaffari SH. An overview of microRNAs: biology, functions, therapeutics, and analysis methods. *J Cell Physiol* 2019;**234**:5451–65.

[18] Hayes J, Peruzzi PP, Lawler S. MicroRNAs in cancer: biomarkers, functions and therapy. *Trends Mol Med* 2014;**20**:460–9.

[19] Jia L, Liu W, Cao B, Li H, Yin C. MiR-507 inhibits the migration and invasion of human breast cancer cells through Flt-1 suppression. *Oncotarget* 2016;**7**:36743–54.

[20] Lv HL, Li ZL, Song YB. MicroRNA-507 represses the malignant behaviors of non-small cell lung cancer via targeting zinc finger E-box binding homeobox 2. *Eur Rev Med Pharmacol Sci* 2019;**23**:9955–64.

[21] Yang Y, Sun KK, Shen XJ, Wu XY, Li DC. miR-557 inhibits the proliferation and invasion of pancreatic cancer cells by targeting EGFR. *Int J Clin Exp Pathol* 2019;**12**:1333–41.

[22] Qiu J, Hao Y, Huang S, Ma Y, Li X, Li D, Mao Y. MiR-557 works as a tumor suppressor in human lung cancers by negatively regulating LEF1 expression. *Tumour Biol* 2017;**39**:1010428317709467.

[23] Wu RR, Zhong Q, Liu HF, Liu SB. Role of miR-579-3p in the development of squamous cell lung carcinoma and the regulatory mechanisms. *Eur Rev Med Pharmacol Sci* 2019;**23**:9464–70.

[24] Schwarzenbacher D, Klec C, Pasculli B, Cerk S, Rinner B, Karbiener M, Ivan C, Barbano R, Ling H, Wulf-Goldenberg A, et al. MiR-1287-5p inhibits triple negative breast cancer growth by interaction with phosphoinositide 3-kinase CB, thereby sensitizing cells for PI3Kinase inhibitors. *Breast Cancer Res* 2019;**21**:20.

[25] Lu J, Tang L, Xu Y, Ge K, Huang J, Gu M, Zhong J, Huang Q. Mir-1287 suppresses the proliferation, invasion, and migration in hepatocellular carcinoma by targeting PIK3R3. *J Cell Biochem* 2018;**119**:9229–38.

[26] Moreno CS. SOX4: the unappreciated oncogene. *Semin Cancer Biol* 2020;**67**:57–64.

[27] Castillo SD, Matheu A, Mariani N, Carretero J, Lopez-Rios F, Lovell-Badge R, Sanchez-Cespedes M. Novel transcriptional targets of the SRY-HMG box transcription factor SOX4 link its expression to the development of small cell lung cancer. *Cancer Res* 2012;**72**:176–86.

[28] Zhang J, Liang Q, Lei Y, Yao M, Li L, Gao X, Feng J, Zhang Y, Gao H, Liu DX, et al. SOX4 induces epithelial-mesenchymal transition and contributes to breast cancer progression. *Cancer Res* 2012;**72**:4597–608.

[29] Wang L, Li Y, Yang X, Yuan H, Li X, Qi M, Chang YW, Wang C, Fu W, Yang M, et al. ERG-SOX4 interaction promotes epithelial-mesenchymal transition in prostate cancer cells. *Prostate* 2014;**74**:647–58.

[30] Wang L, Zhang J, Yang X, Chang YW, Qi M, Zhou Z, Han B. SOX4 is associated with poor prognosis in prostate cancer and promotes epithelial-mesenchymal transition in vitro. *Prostate Cancer Prostatic Dis* 2013;**16**:301–7.

[31] Zhang H, Alberich-Jorda M, Amabile G, Yang H, Staber PB, Di Ruscio A, Welner RS, Ebralidze A, Zhang J, Levantini E, et al. Sox4 is a key oncogenic target in C/EBPalpha mutant acute myeloid leukemia. *Cancer Cell* 2013;**24**:575–88.

[32] Huang HY, Cheng YY, Liao WC, Tien YW, Yang CH, Hsu SM, Huang PH. SOX4 transcriptionally regulates multiple SEMA3/plexin family members and promotes tumor growth in pancreatic cancer. *PLoS One* 2012;**7**:e48637.

[33] Saegusa M, Hashimura M, Kuwata T. Sox4 functions as a positive regulator of beta-catenin signaling through upregulation of TCF4 during morular differentiation of endometrial carcinomas. *Lab Invest* 2012;**92**:511–21.

[34] Cheng Q, Du J, Xie L, Liu X, Li Z, Zuo F, Wu J, Xu J. Inhibition of SOX4 induces melanoma cell apoptosis via downregulation of NF-kappaB p65 signaling. *Oncol Rep* 2018;**40**:369–76.

[35] Wang D, Hao T, Pan Y, Qian X, Zhou D. Increased expression of SOX4 is a biomarker for malignant status and poor prognosis in patients with non-small cell lung cancer. *Mol Cell Biochem* 2015;**402**:75–82.

[36] Li D, He C, Wang J, Wang Y, Bu J, Kong X, Sun D. MicroRNA-138 inhibits cell growth, invasion, and EMT of non-small cell lung cancer via SOX4/p53 feedback loop. *Oncol Res* 2018;**26**:385–400.

[37] Zhou Y, Wang X, Huang Y, Chen Y, Zhao G, Yao Q, Jin C, Liu X, Li G. Down-regulated SOX4 expression suppresses cell proliferation, metastasis and induces apoptosis in Xuanwei female lung cancer patients. *J Cell Biochem* 2015;**116**:1007–18.

[38] Hu WB, Wang L, Huang XR, Li F. MicroRNA-204 targets SOX4 to inhibit metastasis of lung adenocarcinoma. *Eur Rev Med Pharmacol Sci* 2019;**23**:1553–62.